

Acute toxicity test under optimal conditions of two commercial reactive dyes using the Fenton-like process: Assessment of process factors by Box–Behnken design

Natwat Srikhao

Khon Kaen University

Arthit Neramittagapong (✉ artner@kku.ac.th)

Khon Kaen University <https://orcid.org/0000-0002-7420-2196>

Pongsert Sriprom

King Mongkut's Institute of Technology Ladkrabang

Sutasinee Neramittagapong

Khon Kaen University

Somnuk Theerakulpisut

Khon Kaen University

Nurak Grisdanurak

Thammasat University

Research Article

Keywords: freshwater fairy shrimps, immobilization, iron powder, commercial reactive dye, decolorization, response surface methodology

Posted Date: February 15th, 2021

DOI: <https://doi.org/10.21203/rs.3.rs-164955/v1>

License:  This work is licensed under a Creative Commons Attribution 4.0 International License.

[Read Full License](#)

1 **Acute toxicity test under optimal conditions of two commercial reactive dyes using the Fenton-like process:**

2 **Assessment of process factors by Box–Behnken design**

3 Natwat Srikhao^{1,2}, Arthit Neramittagapong^{1,2,*}, Pongsert Sriprom³,

4 Sutasinee Neramittagapong^{1,2}, Somnuk Theerakulpisut⁴, Nurak Grisdanurak⁵

5 ¹ Department of Chemical Engineering, Faculty of Engineering, Khon Kaen University,

6 Khon Kaen 40002, Thailand

7 ² Research Center for Environmental and Hazardous Substance Management (EHSM),

8 Khon Kaen University, Khon Kaen 40002, Thailand

9 ³ Program of Food Processing Engineering, Faculty of Agro-Industry,

10 King Mongkut's Institute of Technology Ladkrabang, Ladkrabang, Bangkok 10520, Thailand

11 ⁴ Energy Management and Conservation Office, Faculty of Engineering, Khon Kaen University, Khon Kaen, 40002,

12 Thailand

13 ⁵ Department of Chemical Engineering, Faculty of Engineering, Thammasat University, Pathumthani, 12000,

14 Thailand

15

16

17

18

19

20

21

22

23

24

25

26

27

28

29

30

31

32

33

34

35

36

Abstract

Reactive dye has generally been used in woven cotton fabric dyeing industries. Some treatments of several reactive dyes may produce more toxicity than the original dyes. The objectives of this study were to find the optimal condition on dye degradation efficiency of commercial reactive red dye 36 (DR36) and reactive violet dye 30 (DV30) using Fenton-like reaction, and to determine acute toxicity by static bioassay method under the optimal condition. The experiment was designed by Box Behnken Design (BBD), in which an initial pH, catalyst dosage and initial concentration of H₂O₂ were considered as independent variables. The results showed that only an initial pH solution was the principal parameter which influenced decolorization of the reactive dyes. Other factors were much less significant. The optimal conditions were found to be given by pH 3, 1 g/L of catalyst dosage, 27.63 mM of concentration of H₂O₂ for DR36, and pH 3, 1.35 g/L of catalyst dosage, 45 mM of concentration of H₂O₂ for DV30. Ninety percent of both decolorization were achieved in 30 min. Acute toxicity tests of the treated solutions using freshwater fairy shrimps (*Streptocephalus sirindhornae*) revealed that the shrimps survived longer than 24 h, indicating that the treated solutions were not acutely toxic. The average leaked iron, ADMI value and total organic carbon were found to be less than 10 ppm, 5 ADMI and 9.17 ppm respectively, in the treated samples. This research demonstrated an efficient method for decolorization of the reactive dyes with low acute toxicity.

Keywords: freshwater fairy shrimps, immobilization, iron powder, commercial reactive dye, decolorization, response surface methodology

*Corresponding author E-mail: artner@kku.ac.th (Arthit Neramittagapong)

70

71 1.Introduction

72 Global textile industries have grown unstopably for several decades, more over 700,000 ton of about 10,000
73 types of dyes and pigments were annually produced (Lyu et al. 2016; Holkar et al. 2016). Consequently, dye, especially
74 reactive dye, has become an important feedstock used in the industry. Since dye cannot be consumed totally in the
75 dyeing process, the unreacted dye could remain in the wastewater discharge, causing the wastewater to have
76 unpleasant appearance and toxicity. In Thailand it has been regulated that wastewater discharge should contain dye
77 concentration less than 300 ppm (Nidheesh et al. 2018) and/or the color of the wastewater should be less than 300
78 ADMI unit. Some reactive dyes were also declared as high toxins promoting *carcinogenesis* and *mutagenesis* (Nasuha
79 et al. 2016; Mahmood Reza Sohrabi et al. 2016).

80 To meet all the requirements of wastewater, several techniques have been used to reduce dye concentration
81 before the wastewater can be discharged. Advanced oxidation processes (AOP) are some promising methods used for
82 the purpose. These processes have been classified as photo-catalytic (Ayyob et al. 2020), ozonation (Powar et al.
83 2020), and Fenton reaction (Ertugay & Acar 2017). Among the AOPs, the Fenton reaction can extensively be used to
84 decompose hard biodegradable organics, including different dyes (Nasuha et al. 2016; Youssef et al. 2016), and textile
85 discharge (Ghanbari et al. 2014; Punzi et al. 2015). The reaction involves a reaction of ferrous ion with H_2O_2 to
86 produce OH^\bullet free radicals having extremely strong oxidation capacity, especially in narrow pH range of 2.8-3.0
87 (Ghanbari et al. 2014; Glugoski et al. 2017). The narrow pH range makes the Fenton reaction difficult to implment
88 (Wang et al. 2017). The heterogeneous Fenton-like catalytic technique has therefore been used more widely, as has
89 been reported on laterite soil (Khataee et al. 2015), red mud (Dias et al. 2016), montmorillonite clay (Fida et al. 2017),
90 zeolite (Rache et al. 2014) and zero valent iron nanoparticles (Vilardi et al. 2018).

91 Reactive dye such as DR36 and DV30 possesses prominent properties for their stabilities (Malade &
92 Deshannavar 2018) and high level of washing fastness (Nallathambi & Venkateshwarapuram Rengaswami 2017).
93 Nasuha et al. (2016) have studied decolorization of reactive black 5 using Fenton-like. Initial dye concentration,
94 hydrogen peroxide concentration, initial pH of a solution and amount of initial catalyst were selected as the main
95 factors for studying this reaction. Khataee et al. (2016) have also studied the effects of operating parameters of the
96 reaction such as catalyst dosages, [pH], [H_2O_2] on their decolorization of Reactive Orange 29 dye. However, the

107 decolorization of these reactive dyes have been studied by considering one factor at a time (OFAT). Interaction effects
108 of the parameters were not studied during the tests.

109 Statistical experimental design could be a better approach in multi-factor study. A systematic study using
110 response surface methodology (RSM), like central composite design (CCD) and Box Behnken Design (BBD), could
111 be used to set up and analyze the experimental data. Some of the advantages of the RMS include its ability to explain
112 both individual and interaction effects, and optimizing decolorization condition. In addition, it's has successfully been
113 applied to various oxidation processes to optimize the experimental design condition (Fu et al. 2009; Berkani et al.
114 2020).

115 In this study, the decolorization of DR36 and DV40 dye was implemented by BBD under three factors
116 simultaneously, including pH, catalyst loading, and amount of H₂O₂. The study was carried out using iron powder in
117 a Fenton-like reaction. The experiment was set up in a range of pH 3-7, Catalyst 0.01-1.5 g/L, and H₂O₂ 0.5-100 mM.
118 The optimum condition and the most influential factor(s) in decolorization of the reactive dyes were the objective of
119 this study. The water after the treatment was also tested for acute toxicity by using fairy shrimps (*Streptocephalus*
120 *sirindhornae*).

121 2. Materials and methods

122 2.1 Materials

123 Reactive red dye 36 (DR36) and violet dye 30 (DV30) (without heavy metal, Dylon, England) used in this
124 study were purchased in Thailand. The Fenton-like experiment were carried out using commercial iron-powder grade
125 (99.64% Gammaco, Thailand). H₂O₂ 30% (QRëC, New Zealand). NaOH (98%wt Ajax Finechem Pty Ltd, Auckland,
126 New Zealand) and H₂SO₄ (96%wt RCI Labscan Limited, Thailand) were used to adjust the solution pH to the desired
127 levels. Ethanol (99.8% Analar NORMAPUR ® ACS, Reag.Ph.Eur. , France) was used to wash the catalyst. Nylon
128 filter membrane (Syring filter 0.45 Micron CNW, China) was used to filter the sample solution before determining
129 the color values using UV-Vis spectrophotometer (SPECORD,Analytik Jena, Germany). All solutions were prepared
130 with deionized water (DI water).

131 2.2 Experimental

124 Iron-powder was sieved to the size range of 100-500 mesh. It was washed by Deionized water and ethanol,
 125 and then dried at 80°C for 1 hour. The obtained material was immediately used right after the preparation. Box–
 126 Behnken design (Software Minitab 16) was used to randomize the experimental values of the three factors at three
 127 levels as shown in Table 1. The studied factors included initial pH, catalyst dosage, and initial concentration of H₂O₂.
 128 The experiments were performed in a batch-wise system of 600 mL container, under room temperature. The
 129 decolorization of reactive dye (300 ppm) was carried out using different initial concentrations of H₂O₂ (0.5-100 mM),
 130 the catalyst dosage (0.01-1.5 g/L) and pH (3-7). One molar of H₂SO₄ or NaOH solution was used to adjust the solution
 131 pH.

132 During the test, the remaining concentration of the reactive dye in the solution was withdrawn 30 minutes
 133 after the beginning of the experiment, and analyzed for the percentage of decolorization efficiency (DE%) and the
 134 American Dye Manufacturers Institute (ADMI) value by UV-Vis spectrophotometer. The Non-Purgeable Organic
 135 Carbon (NPOC) method was used to determine the TOC value. These values were compared with those of the solution
 136 withdrawn prior to the commencement of the experiment.

137 The catalyst was further characterized for its surface area and composition by N₂ Adsorption-Desorption
 138 (ASAP 2010, Micromeritics, USA) and X-Ray Fluorescence Spectrometry (SEA1000A, Seiko Instruments GmbH,
 139 Germany), respectively. After 30 minutes of reaction, the solution was analyzed for iron leachate by Inductively
 140 Coupled Plasma-Optical Emission Spectrometer (Optima 8x00 Series, PerkinElmer, United States of America).

141

142 **Table 1** Box-Behnken design for varying the factors

Factors	Symbol	Levels of factors		
		-1	0	1
Initial pH	(X ₁)	3	5	7
Catalyst dosage (g/L)	(X ₂)	0.01	0.755	1.5
Initial concentration of H ₂ O ₂ (mM)	(X ₃)	0.5	50.25	100

143

144 The Quadratic polynomial model equation (1) was obtained to analyze the data using the least square of error
 145 technique as follows:

$$146 \quad Y = \beta_0 + \beta_1 X_1 + \beta_2 X_2 + \beta_3 X_3 + \beta_4 X_1^2 + \beta_5 X_2^2 + \beta_6 X_3^2 + \beta_7 X_1 X_2 + \beta_8 X_1 X_3 + \beta_9 X_2 X_3 \pm \varepsilon \quad (1)$$

147 In which Y is dye removal efficiency (response function), β_i are regression coefficient, X_i are independent
 148 variables, and ε is value of the error.

149
150 2.3 Acute toxicity assays

151 Young freshwater fairy shrimps (*Streptocephalus sirindhornae Sanoamuang*) were obtained from a stock
152 maintained at the Department of Fisheries, Khon Kaen University. The acute toxicity and immobilization tests were
153 performed according to 202 of OECD Guidelines for Testing of Chemicals (OCDE, 1984) with modifications. For the
154 tests, 20 of neonates were divided into five groups of four animals each. The first and second groups were exposed to
155 both (DR36 and DV30) of the original dye diffusion (300 mg/L), the third and fourth groups in the treated water from
156 the optimal condition in Fenton-like process (DR36 and DV30), and the final group in the water obtained from the
157 source of fairy shrimps (control water).

158 The water obtained from the source of fairy shrimp culture was used as the control water. The acute toxicity
159 assays can be assessed by counting the number of dead and surviving neonates at 0.5, 1, 6, 12, 24, 36, 48, 60 hours
160 and compared with the control water. Prior to the test, the solution of every experimental batch was adjusted to the
161 pH value of 7.66 before adding the neonates except the control water. This experiment did not have any light control.
162 Therefore, the daytime was assumed to be approximately 12h, and 12h nighttime.

163
164 3. Results and discussion

165 3.1 Characteristics of catalysts

166 The specific surface area was determined to be 3.932 m²/g by the Brunauer–Emmett–Teller (BET) method
167 using the N₂ Adsorption-Desorption Semisorb, (ASAP 2010, Micromeritics, USA). The purity of the iron-powder was
168 found to be 99.64%wt using X-Ray Fluorescence Spectrometry.

169
170 3.2 Dye degradation

171 The values of dependent and independent factors, and the condition for every experimental data set which was
172 obtained from Box–Behnken design (Table 1) are presented in Table 2. The decolorization efficiency (DE%) of DR36
173 and DV30 were calculated by Equation 2 and shown in Table 2.

174
$$DE\% = \frac{c_0 - c_t}{c_0} \times 100 \quad (2)$$

175 where DE% is the decolorization efficiency, C₀ is the initial concentration of the dye, and C_t is concentration of the
176 dye at 30 min.

177

178 **Table 2** Results of the Box–Behnken experimental design for dye decolorization efficiency
 179 (DE%) of DR36 and DV30.
 180

Run	Initial pH	Catalyst dosage (g/L)	H ₂ O ₂ (mM)	%DE of DR36 dye 30 min	%DE of DV30 dye 30 min
1	5	0.01	0.5	19.523	24.945
2	3	0.01	50.25	42.668	78.061
3	7	0.01	50.25	7.768	10.950
4	3	0.755	0.5	99.244	94.770
5	5	0.01	100	19.994	22.047
6	7	0.755	0.5	21.411	10.833
7	5	1.5	0.5	39.764	64.757
8	7	1.5	50.25	22.460	25.771
9	3	1.5	50.25	94.033	77.113
10	7	0.755	100	19.144	4.785
11	5	1.5	100	45.714	93.609
12	5	0.755	50.25	62.514	64.182
13	5	0.755	50.25	62.796	81.096
14	5	0.755	50.25	53.157	64.208
15	3	0.755	100	92.751	62.056

181
 182 The coefficients of the response functions for various independent variables were obtained by correlating the
 183 experimental results with the response functions by using a Minitab 16 statistical software. The response functions for
 184 DR36 and DV30 were obtained by the Least Square of Error method as Equations 3 and 4, respectively for predicting
 185 the dye decolorization efficiency.

186
$$\%Y(DR36) = 55.43 - 30.25X_1 + 9.70X_2 - 3.9X_3 - 1.62X_1^2 - 20.06X_2^2 - 7.01X_3^2 - 8.21X_1X_2 + 3.34X_1X_3 +$$

 187
$$1.76X_2X_3 \quad (3)$$

188
 189
$$\%Y(DR36) = 69.83 - 32.46X_1 + 15.66X_2 - 1.6X_3 - 15.04X_1^2 - 6.81X_2^2 - 11.68X_3^2 + 3.94X_1X_2 + 6.67X_1X_3 +$$

 190
$$7.94X_2X_3 \quad (4)$$

 191

192 Figure 1 and 2 can be used to verify the accuracy of Equations 3 and 4, respectively. Figures 1a and 2a indicate
 193 that the data were distributed on straight lines independently. Figure 1B and 2B show the stability of variance to be
 194 dispersed around the zero. The histogram of the Figure 1C and 2C demonstrate that the standard deviation of the data
 195 was well distributed (bell-shape) and tend to the center. Lastly, Figure 1D and 2D show the standardized residual of
 196 the data with respect to the observation order. These two figures reveal that the order of the experiment was well
 197 distributed, indicating that the experimental design was well randomized.

198

199

200

201

202

203

204

205

206

207

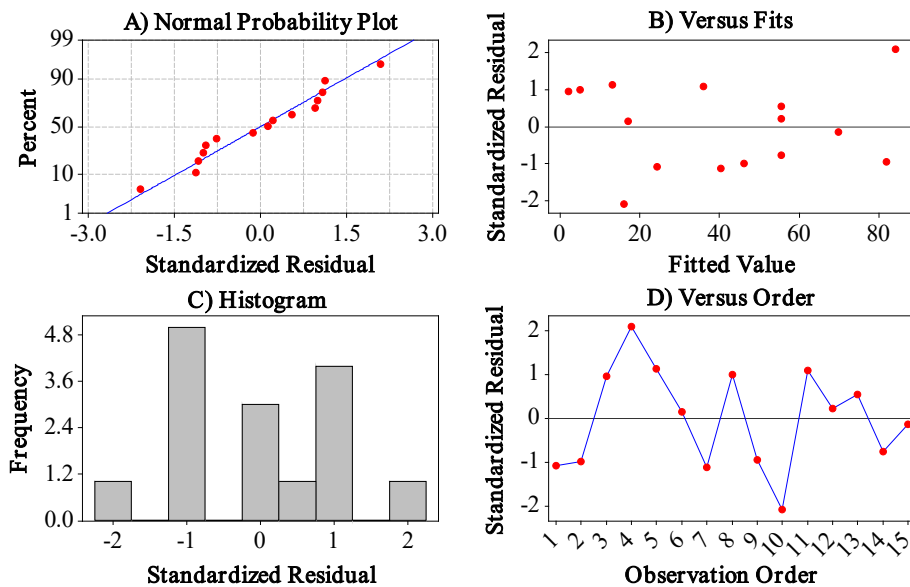
208

209

210

211

212



213 Fig. 1 Standard error compared to a) standardized residual b) versus fits c) Histogram d) Versus order.

214

215

216

217

218

219

220

221

222

223

224

225

226

227

228

229
 230
 231
 232
 233
 234
 235
 236
 237
 238
 239
 240
 241
 242
 243
 244
 245
 246
 247
 248
 249
 250
 251
 252
 253
 254
 255
 256
 257
 258
 259
 260
 261
 262

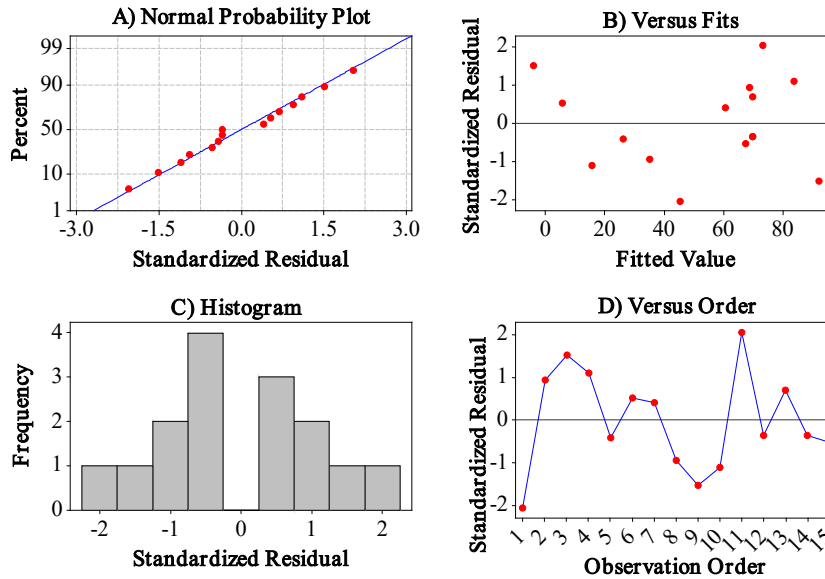


Fig. 2 Standard error compared to A) standardized residual B) versus fits C) Histogram D) Versus Order.
 For DV30.

Based on the statistical data of Figures 1 and 2, it can be seen that the data obtained were well distributed and independent. In other words, no abnormal statistical data were observed. Therefore, Equations 3 and 4 can be used with some degree of confidence. Equations 3 and 4 were also analysed for variance by ANOVA test with 95% confidence interval. The F_{value} and P_{value} were considered for each variable presented in Table 3.

From Table 3, it should be noted that only terms of linear source, which have statistically significant effects on the DE% of DR36 and DV30. For DR36, the significant factors were found to be initial pH (X_1), the catalyst dosage (X_2) and the term of X_2^2 . Even though the initial concentration of hydrogen peroxide (X_3) was not significant, it is necessary for a Fenton-like reaction as the reducing agent. For DV30, it was found that only the initial pH was the significant factor, while other factors were insignificant, but they were needed for the reaction.

However, the applicability of Equations 3 and 4 must be judged by the term of Lack of fit which is used to indicate to the error of these equations. Table 3 shows that the Lack of fit values for DR36 and DV30 were not significant. Therefore, the equations are statistically reliable without a need to remove any factors from the equations (Ay et al. 2009), indicating the model can be used to forecast the DE%.

263 **Table 3** ANOVA test for response function Y (DE%)

Source	DF	DR36			DV30		
		F-value	P-value	Result	F-value	P-value	Result
Regression	9	10.71	0.009	Significant	3.46	0.093	Insignificant
Linear	3	26.03	0.002	Significant	8.82	0.019	Significant
X ₁	1	69.76	0.000	Significant	21.42	0.006	Significant
X ₂	1	7.18	0.044	Significant	4.98	0.076	Insignificant
X ₃	1	1.16	0.331	Insignificant	0.05	0.828	Insignificant
Square	3	5.07	0.056	Insignificant	1.13	0.420	Insignificant
X ₁ ²	1	0.09	0.774	Insignificant	2.12	0.205	Insignificant
X ₂ ²	1	14.15	0.013	Significant	0.44	0.538	Insignificant
X ₃ ²	1	1.73	0.246	Insignificant	1.28	0.309	Insignificant
Interaction	3	1.03	0.453	Insignificant	0.42	0.749	Insignificant
X ₁ × X ₂	1	2.57	0.170	Insignificant	0.16	0.707	Insignificant
X ₁ × X ₃	1	0.42	0.543	Insignificant	0.45	0.531	Insignificant
X ₂ × X ₃	1	0.11	0.751	Insignificant	0.64	0.460	Insignificant
Residual	5						
Error							
Lace-of-fit	3	4.71	0.180	Insignificant	6.22	0.142	Insignificant
Pure-Error	2						
Total	14						

264 F-test 95% confidence ($\alpha=0.05$)

Source	DF 1	DF 2	F critical
F _(0.05,DF1,DF2)	9	5	4.77
F _(0.05,DF1,DF2)	3	5	5.41
F _(0.05,DF1,DF2)	1	5	6.61
F _(0.05,DF1,DF2)	3	2	19.16

265

266 Comparison between the predicted and experimental values can be made by plotting the predicted values
 267 against the experimental values as shown in Fig.3A and 3B for DR36 and DV30, respectively. As shown in Fig. 3A,
 268 the equation obtained fits approximately well with experimental results (less than 10% error). Similarly, Fig 3B reveals
 269 similar results but with less accuracy (less than 15% error). It should be noted, however, for the range of 70- 80% of
 270 decolorization the model for DV30 can be used to predict decolorization with improved accuracy (less than 10%
 271 error). Consequently, it can be concluded that both of the models were in reasonably good agreement with the
 272 experiment.

273

274

275

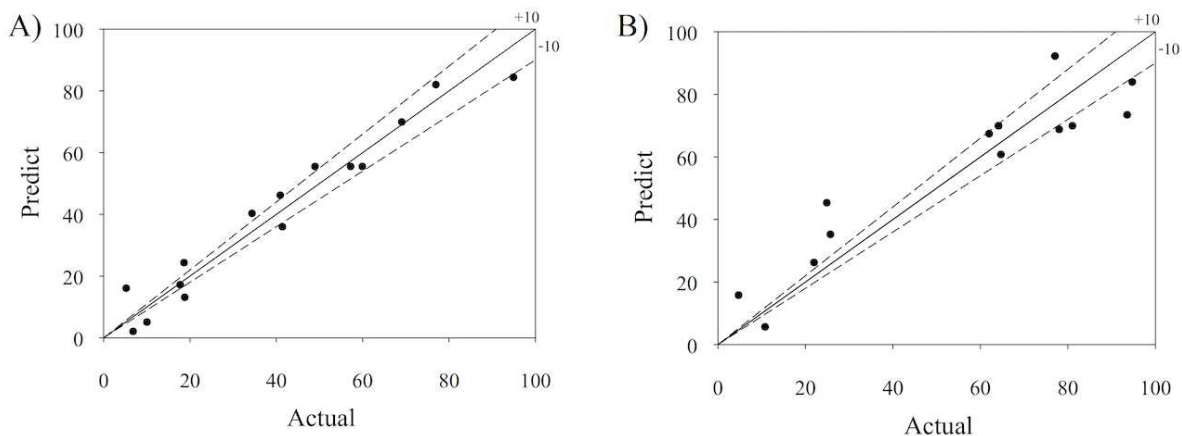


Fig. 3. Experimental and predicted equation results for decolorization A) DR36 B) DV30

3.3 Effects of parameters on decolorization efficiency

The initial pH (X_1) was found to be the most influential factor on the decolorization efficiency. The F-value can confirm this in Table 3 where the F_{value} values were found to be 69.76 and 21.42 for DR36 and DV30, respectively. On the contrary, the catalyst dosage (X_2) and the initial concentration of H_2O_2 (X_3) were much less influential on decolorization.

More interestingly, based on statistical results in Table 3, it should be noted that the interaction effects between the insignificant variables and significant variables were not significant. However, the interaction effects of the variables were shown to influence decolorization by response surface methodology (Fig.4).

The interaction effects of between (X_1) and (X_2) were depicted in Fig. 4A and Fig.4D, whereas Fig. 4B and Fig. 4E show the interaction effects between (X_1) and (X_3). It is seen that %DE increases with the catalyst dosage and H_2O_2 at a constant pH of 3. At other pH values, the %DE is slightly affected by the catalyst dosage and initial concentration of H_2O_2 . At the initial pH of 3, the decolorization efficiency is the highest. This finding was also observed by Khataee et al. (2015), who used the iron-rich laterite soil as the catalyst. This can be explained by the instability of H_2O_2 and depressed oxidation potential of hydroxyl radicals at higher pH (Fida et al., 2017). In addition, the alkaline solution causes the Ferrous ion (Fe^{2+}) to transform to be Iron (II) hydroxide ($Fe(OH)_2$) according to Equation 5. Fe in this form is inactive (Ertugay & Acar 2017; Chu et al. 2012).



309
310
311 Fig. 4C and Fig. 4F show the DE% tends to the maximum value as X_2 and X_3 increase until some limits. The
312 limits of X_2 were found to be 1.3g/l for DR36 and 1.5g/l for DV30. The limits were due to excessive active sites of
313 the catalyst, resulting in excessive ferrous ions (Khataee et al., 2015; Fida et al., 2017). In theory, the ferrous ion can
314 react with H_2O_2 to produce more hydroxyl radicals (Khataee et al. 2015; Ma et al. 2015), but excessive ferrous ions
315 will result in some of the ions becoming the scavengers of the hydroxyl radicals (Li et al. 2017; Bouzayani et al. 2017)
316 as illustrated in Equations 6-8.



320 where X is the solid catalyst support.

321 In a similar manner to the catalyst dosage, the DE% increases with H_2O_2 concentration until some limits. The
322 H_2O_2 concentration over 60 mM tends to decrease the DE%. Excessive H_2O_2 will result in hydroxyl radical scavenging
323 (Mahmood R. Sohrabi et al., 2017; Quadrado & Fajardo, 2017; Grisales et al., 2019) according to Equations 9 and 10.



324
325
326
327 In conclusion, the study of the effects of the parameters on decolorization efficiency, as presented in Figure 4,
328 reveals that the most influential parameter is the initial pH, which should be controlled at pH 3 for the best dye
329 decolorization efficiency. The other factors, namely catalyst dosage and concentration of H_2O_2 , should respectively
330 be kept in the ranges of 0.9-1.2 g/L, and 20-35 mM of $[H_2O_2]$ for DR36, and 1.3-1.5 g/L, and 40-50 mM of $[H_2O_2]$
331 for DV30.

332

333

334

335

336

337

338

339

340

341

342

343

344

345

346

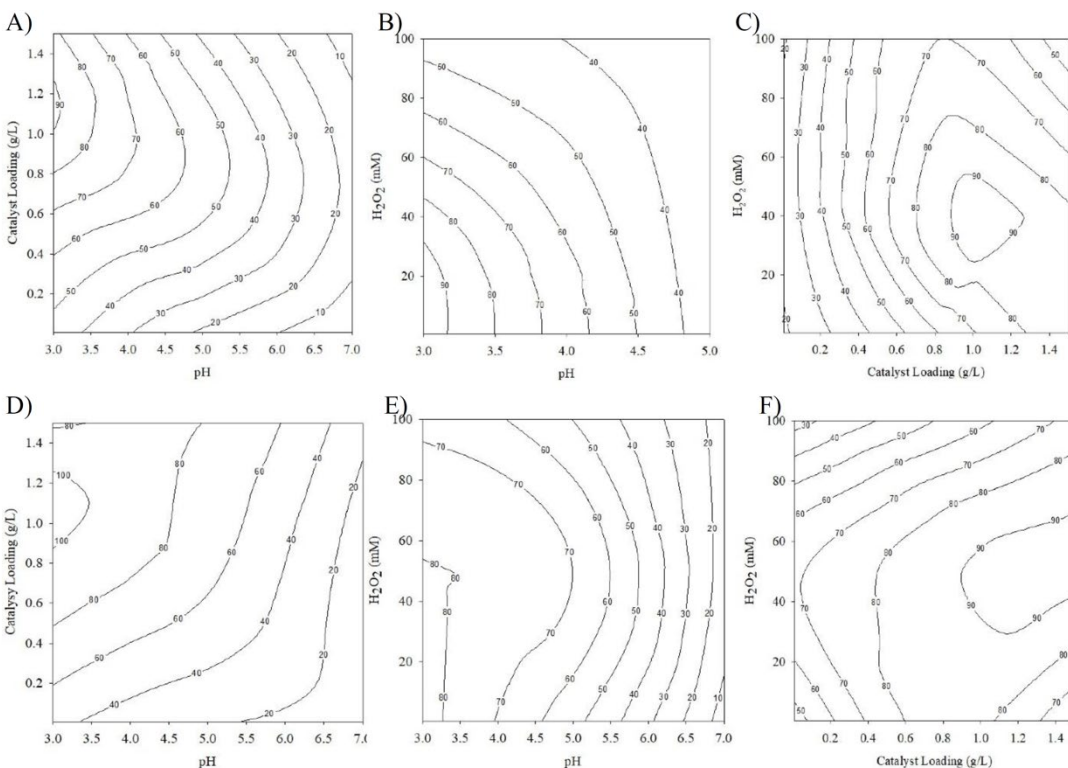
347

348

349

350

351



352 Fig. 4 Contour plot illustrations, the interaction effect of variables on dye decolorization efficiency in
 353 the Fenton -like process in white (A-C) For DR36 and (D-F) for DV30.

354

355 3.4 Optimal condition and asseveration of the findings

356 The optimal conditions of dyes were predicted by using Equations 3 and 4 for DR36 and DV30, respectively.

357 These equations were obtained by the Least Square method based on the numerical values generated from the

358 experimental data by Minitab 16 software. The optimal conditions were found to be pH 3, 1 g/L of catalyst dosage,

359 27.63 mM of H₂O₂ For DR36, and pH 3, 1.35 g/L of catalyst dosage, 45 mM of H₂O₂ for DV30. Under these predicted

360 conditions, the best of DE% were found to be 89.38% and 92.33% for DR36 and DV30, respectively.

361 In order to verify the accuracy of the optimal conditions, three decolorization tests were repeated for DR36 and

362 three tests for DV30. The average experimental results of DE% were 91.86% with a standard deviation of 7.24%

363 and 92.97% with a standard deviation of 8.88% for DR36 and DV30, respectively. The experimental results were,

364 therefore, comparable with the predicted values with the standard deviations as described.

365 Furthermore, under these optimal conditions, the average values of leached iron, TOC, and ADMI unit were
 366 also determined. These results were less than 10 ppm, 9.17 ppm, 5 ADMI, respectively. The treated water was
 367 therefore in compliance with American Dye Manufacturing Institute, and Thailand's Industrial Discharge Water
 368 standards.

369

370 3.5 Acute toxicity

371 Fig. 5 shows the results of acute toxicity test of the treated water with the optimal condition. The test was
 372 performed by counting fatalities of the fairy shrimps exposed to the treated water and the original untreated water.
 373 The result showed, after 24 hours, that no deaths were observed in all of the batches. This leads to the conclusion that
 374 there was no difference in acute toxicity of the treated and untreated water.

375 However, when the toxicity test reached 48 h, only 25% of the neonates in the original, untreated water with
 376 DR36 died, whereas the fatalities in the case of DV30 were 27%. In the case of treated waters and cultured water were
 377 found not any death. At 60 h, the treated water showed a slightly better survival rate than the original, untreated water.
 378 The survival rate was found to be 76% for treated waters (both DR36 and DV30), while the original, untreated water
 379 showed 74% and 72% for DR36 and DV30, respectively. No fatality was observed in the control water.

380 In conclusion, only a slight difference in toxicity between the treated and untreated water. Fernandes et al.
 381 (2018). also observed a similar result in their acute toxicity test (24 h). Therefore, the Fenton-like reaction under the
 382 optimal condition could be well applied to treat wastewater from the dyeing industry.

383

384

385

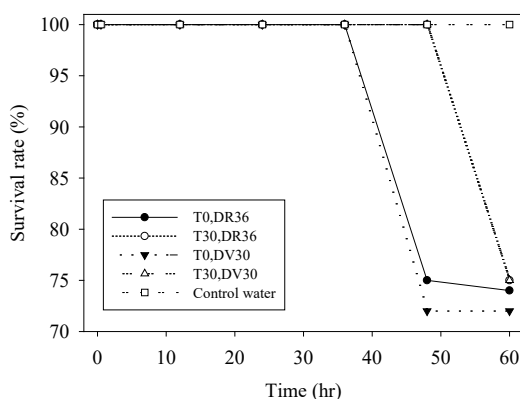
386

387

388

389

390



391 Fig. 5 Effects of different treated water and untreated water with survival rate (%) of fairy shrimp (T0 is

392 original dye at 300 ppm, T30 is treated water, and control water is water from a freshwater fairy shrimp

393 culture.
394

395

396

397

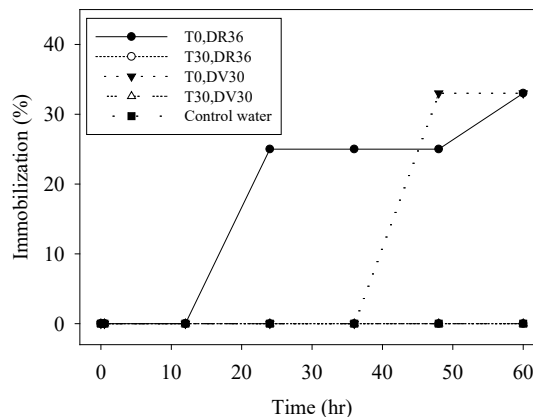
398

399

400

401

402



403 Fig. 6. Effects of different treated water and untreated water with immobilization (%) of fairy shrimp, T0 is
404 original dye at 300 ppm, T30 is treated water, and control water is water from a freshwater fairy
405 shrimp culture
406

407 The immobilization test of the fairy shrimps was also carried out and presented in Fig.6. The test mainly
408 involved observing the movement of the laboratory animals. The experiment result revealed no abnormal movement
409 of the fairy shrimps in the control water and all the treated water. However, only in the untreated water (DR36), 25%
410 of immobilization was observed at 24 h, while in the untreated water (DV30), 33% of immobilization was observed
411 at 48 h. This result indicated the treated water was less harmful to the fairy shrimps than the untreated water.

412

413 4. Conclusion

414 A Box–Behnken design was used to find the optimal condition for dye decolorizing efficiency by considering
415 the three variables, including initial pH, catalyst dosage and initial concentration of hydrogen peroxide. The initial pH
416 was found to be the most influential parameter on dye decolorization efficiency. The Least Square of Error method
417 was used to create the models for predicting the dye decolorizing efficiency for DR36 and DV30, respectively. The
418 model can be used to predict the optimal decolorization conditions for DR36 and DV30. The optimal conditions were
419 experimentally verified, and it was found that the predicted DE% was in good agreement with the experimental values.
420 More importantly, the treated water was in compliance with the American Dye Manufacturing Institute and Thailand's

421 Industrial Wastewater Discharge standards. The toxicity test revealed no acute toxicity. Therefore, the Fenton-like
422 reaction using iron-powder as the catalyst is suitable for removing DR36 and DV30.

423
424 **Acknowledgements**

425 This research was granted by Research Fund of the Faculty of Engineering, Khon Kaen University, Thailand,
426 contract No. 4-1/2559.

427 -Ethical Approval: Compliance with Ethical Standards

428
429 -Consent to Participate: All applicable international, national, and/or institutional guidelines for the care and use of
430 animals were followed.

431
432 -Consent to Publish: Not applicable

433
434 -Authors' Contributions: Natwat Srikhao planed, designed the experiments, collected data, interpreted, analyzed, and
435 wrote a manuscript. Arthit Neramittagapong, Pongsert Sriprom, and Sutasinee Neramittagapong designed the
436 experiments, provided chemicals and instruments, interpreted, analyzed, discussed, and wrote a manuscript. Somnuk
437 Theerakulpisut and Nurak Grisdanurak interpreted, analyzed, discussed, and wrote a manuscript

438
439 -Funding: This study was funded by the Research Fund of the Faculty of Engineering, Khon Kaen University,
440 Thailand, contract No. 4-1/2559.

441
442 -Competing Interests: The authors declare that they have no competing interests.

443
444 -Availability of data and materials: Not applicable

445
446
447 **Reference**

448
449 Ay F, Catalkaya EC, Kargi F (2009) A statistical experiment design approach for advanced oxidation of Direct Red
450 azo-dye by photo-Fenton treatment. *J Hazard Mater* 162:230–236.

451 <https://doi.org/10.1016/j.jhazmat.2008.05.027>

452 Ayyob M, Ahmad I, Hussain F, Kashif Bangash M, Awan JA, Jaubert JN (2020) A new technique for the synthesis
453 of lanthanum substituted nickel cobaltite nanocomposites for the photo catalytic degradation of organic dyes
454 in wastewater. *Arab J Chem* 12:6341-6347. <https://doi.org/10.1016/j.arabjc.2020.05.036>

455 Berkani M, Kadmi Y, Bouchareb MK, Bouhelassa M, Bouzaza A (2020) Combination of a Box-Behnken design
456 technique with response surface methodology for optimization of the photocatalytic mineralization of C.I.
457 Basic Red 46 dye from aqueous solution. *Arab J Chem* <https://doi.org/10.1016/j.arabjc.2020.05.013>

- 458 Bouzayani B, Meijide J, Pazos M, Elaoud SC, Sanroman MA (2017) Removal of polyvinylamine sulfonate
459 anthrapyridone dye by application of heterogeneous electro-Fenton process. *Environ Sci Pollut Res* 24:18309–
460 18319. <https://doi.org/10.1007/s11356-017-9468-5>
- 461 Chu L, Wang J, Dong J, Liu H, Sun X (2012) Treatment of coking wastewater by an advanced Fenton oxidation
462 process using iron powder and hydrogen peroxide. *Chemosphere* 86:409–414.
463 <https://doi.org/10.1016/j.chemosphere.2011.09.007>
- 464 Dias FF, Oliveira AAS, Arcanjo AP, Moura FCC, Pacheco JGA (2016) Residue-based iron catalyst for the
465 degradation of textile dye via heterogeneous photo-Fenton. *Appl Catal B Environ* 186:136–142.
466 <https://doi.org/10.1016/j.apcatb.2015.12.049>
- 467 Ertugay N, Acar FN (2017) Removal of COD and color from Direct Blue 71 azo dye wastewater by Fenton's
468 oxidation: Kinetic study. *Arab J Chem* 10:S1158–S1163. <https://doi.org/10.1016/j.arabjc.2013.02.009>
- 469 Fernandes NC, Brito LB, Costa GG, Taveira SF, Cunha-Filho MSS, Oliveira GAR, Marreto RN (2018) Removal of
470 azo dye using Fenton and Fenton-like processes: Evaluation of process factors by Box–Behnken design and
471 ecotoxicity tests. *Chem Biol Interact* 291:47–54. <https://doi.org/10.1016/j.cbi.2018.06.003>
- 472 Fida H, Zhang G, Guo, Naeem A (2017) Heterogeneous Fenton degradation of organic dyes in batch and fixed bed
473 using La-Fe montmorillonite as catalyst. *J Colloid Interface Sci* 490:859–868.
474 <https://doi.org/10.1016/j.jcis.2016.11.085>
- 475 Fu JF, Zhao YQ, Xue XD, Li WC, Babatunde AO (2009) Multivariate-parameter optimization of acid blue-7
476 wastewater treatment by Ti/TiO₂ photoelectrocatalysis via the Box–Behnken design. *Desalination* 243:42–51.
477 <https://doi.org/10.1016/j.desal.2008.03.038>
- 478 Ghanbari F, Moradi M, Manshouri M (2014) Textile wastewater decolorization by zero valent iron activated
479 peroxymonosulfate: Compared with zero valent copper. *J Environ Chem Eng* 2:1846–1851.
480 <https://doi.org/10.1016/j.jece.2014.08.003>
- 481 Glugoski LP, Cubas PDJ, Fujiwara ST (2017) Reactive Black 5 dye degradation using filters of smuggled cigarette
482 modified with Fe³⁺. *Environ Sci Pollut Res* 24:6143–6150.
483 <https://doi.org/10.1007/s11356-016-6820-0>
- 484 Grisales CM, Salazar LM, Garcia DP (2019) Treatment of synthetic dye baths by Fenton processes: evaluation of
485 their environmental footprint through life cycle assessment. *Environ Sci Pollut Res* 26:4300–4311.
486 <https://doi.org/10.1007/s11356-018-2757-9>
- 487 Holkar CR, Jadhav AJ, Pinjari DV, Mahamuni NM, Pandit AB (2016) A critical review on textile wastewater
488 treatments: Possible approaches. *J Environ Manage* 182:351–366.
489 <https://doi.org/10.1016/j.jenvman.2016.07.090>
- 490 Khataee A, Gholami P, Sheydaei M (2016) Heterogeneous Fenton process by natural pyrite for removal of a textile
491 dye from water: Effect of parameters and intermediate identification. *J Taiwan Inst Chem Eng* 58:366–373.
492 <https://doi.org/10.1016/j.jtice.2015.06.015>
- 493 Khataee A, Salahpour F, Fathinia M, Seyyedi B, Vahid B (2015) Iron rich laterite soil with mesoporous structure for
494 heterogeneous Fenton-like degradation of an azo dye under visible light. *J Ind Eng Chem* 26:129–135.

- 495 <https://doi.org/10.1016/j.jiec.2014.11.024>
- 496 Li K, Zhao Y, Janik MJ, Song C, Guo X (2017) Facile preparation of magnetic mesoporous Fe₃O₄/C/Cu composites
497 as high performance Fenton-like catalysts. *Appl Surf Sci* 396:1383–1392.
498 <https://doi.org/10.1016/j.apsusc.2016.11.170>
- 499 Lyu C, Zhou D, Wang J (2016) Removal of multi-dye wastewater by the novel integrated adsorption and Fenton
500 oxidation process in a fluidized bed reactor. *Environ Sci Pollut Res* 23:20893–20903.
501 <https://doi.org/10.1007/s11356-016-7272-2>
- 502 Ma J, Zhou L, Dan W, Zhang H, Shao Y, Bao C, Jing L (2015) Novel magnetic porous carbon spheres derived from
503 chelating resin as a heterogeneous Fenton catalyst for the removal of methylene blue from aqueous solution. *J*
504 *Colloid Interface Sci* 446:298–306. <https://doi.org/10.1016/j.jcis.2015.01.036>
- 505 Malade LV, Deshannavar UB (2018) Decolorisation of Reactive Red 120 by hydrodynamic cavitation. *Mater Today*
506 *Proc* 5:18400–18409. <https://doi.org/10.1016/j.matpr.2018.06.180>
- 507 Nallathambi A, Venkateshwarapuram Rengaswami GD (2017) Industrial scale salt-free reactive dyeing of
508 cationized cotton fabric with different reactive dye chemistry. *Carbohydr Polym* 174:137–145.
509 <https://doi.org/10.1016/j.carbpol.2017.06.045>
- 510 Nasuha N, Ismail S, Hameed BH (2016) Activated electric arc furnace slag as an efficient and reusable
511 heterogeneous Fenton-like catalyst for the degradation of Reactive Black 5. *J Taiwan Inst Chem Eng* 67:235–
512 243. <https://doi.org/10.1016/j.jtice.2016.07.023>
- 513 Nidheesh PV, Zhou M, Oturan MA (2018) An overview on the removal of synthetic dyes from water by
514 electrochemical advanced oxidation processes. *Chemosphere* 197:210–227.
515 <https://doi.org/10.1016/j.chemosphere.2017.12.195>
- 516 OCDE Guideline for Testing of Chemical (1984) *Daphnia* sp Acute Immobilisation Test and Reproduction Test.
517 *Guideline*:1–16.
- 518 Powar AS, Perwuelz A, Behary N, Hoang L, Aussenac T (2020) Application of ozone treatment for the
519 decolorization of the reactive-dyed fabrics in a pilot-scale process-optimization through response surface
520 methodology. *Sustain* 12. <https://doi.org/10.3390/su12020471>
- 521 Punzi M, Anbalagan A, Aragão BR, Svensson BM, Jonstrup M, Mattiasson B (2015) Degradation of a textile azo
522 dye using biological treatment followed by photo-Fenton oxidation: Evaluation of toxicity and microbial
523 community structure. *Chem Eng J* 270:290–299. <https://doi.org/10.1016/j.cej.2015.02.042>
- 524 Quadrado RFN, Fajardo AR (2017) Fast decolorization of azo methyl orange via heterogeneous Fenton and Fenton-
525 like reactions using alginate-Fe²⁺/Fe³⁺ films as catalysts. *Carbohydr Polym* 177:443–450.
526 <https://doi.org/10.1016/j.carbpol.2017.08.083>
- 527 Rache ML, García AR, Zea HR, Silva AMT, Madeira LM, Ramírez JH (2014) Azo-dye orange II degradation by the
528 heterogeneous Fenton-like process using a zeolite Y-Fe catalyst—Kinetics with a model based on the Fermi's
529 equation. *Appl Catal B Environ* 146:192–200. <https://doi.org/10.1016/J.APCATB.2013.04.028>
- 530 Sohrabi MR, Khavaran A, Shariati S, Shariati S (2017) Removal of Carmoisine edible dye by Fenton and photo
531 Fenton processes using Taguchi orthogonal array design. *Arab J Chem* 10:S3523–S3531.

- 532 <https://doi.org/10.1016/j.arabjc.2014.02.019>
- 533 Sohrabi MR, Moghri M, Fard Masoumi HR, Amiri S, Moosavi N (2016) Optimization of Reactive Blue 21 removal
534 by Nanoscale Zero-Valent Iron using response surface methodology. Arab J Chem 9:518–525.
535 <https://doi.org/10.1016/j.arabjc.2014.11.060>
- 536 Vilardi G, Di Palma L, Verdone N (2018) On the critical use of zero valent iron nanoparticles and Fenton processes
537 for the treatment of tannery wastewater. J Water Process Eng 22:109–122.
538 <https://doi.org/10.1016/J.JWPE.2018.01.011>
- 539 Wang J, Liu C, Li J, Luo R, Hu X, Sun X, Shen J, Han W, Wang L (2017) In-situ incorporation of iron-copper
540 bimetallic particles in electrospun carbon nanofibers as an efficient Fenton catalyst. Appl Catal B Environ
541 207:316–325. <https://doi.org/10.1016/j.apcatb.2017.02.032>
- 542 Youssef NA, Shaban SA, Ibrahim FA, Mahmoud AS (2016) Degradation of methyl orange using Fenton catalytic
543 reaction. Egypt J Pet 25:317–321. <https://doi.org/10.1016/j.ejpe.2015.07.017>
- 544
- 545

Figures

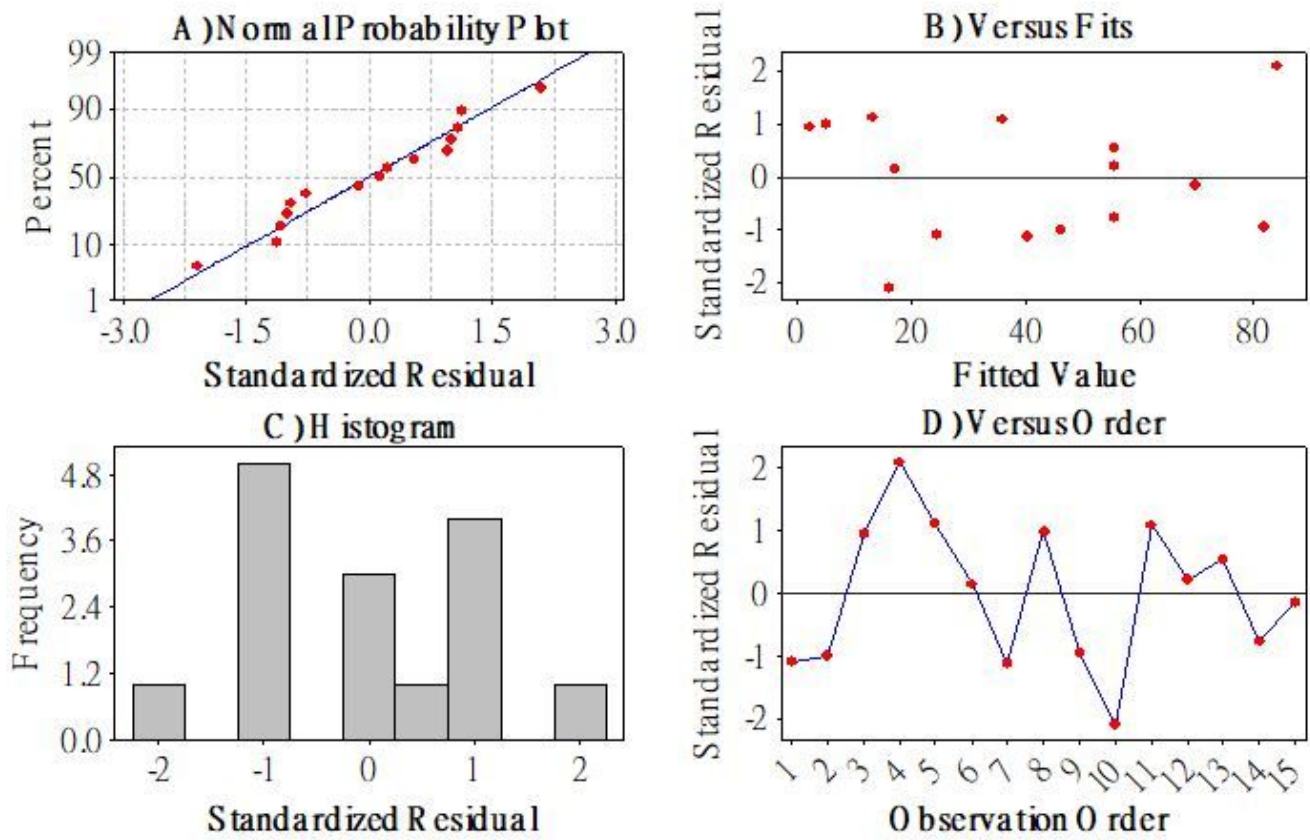


Figure 1

Standard error compared to a) standardized residual b) versus fits c) Histogram d) Versus order.

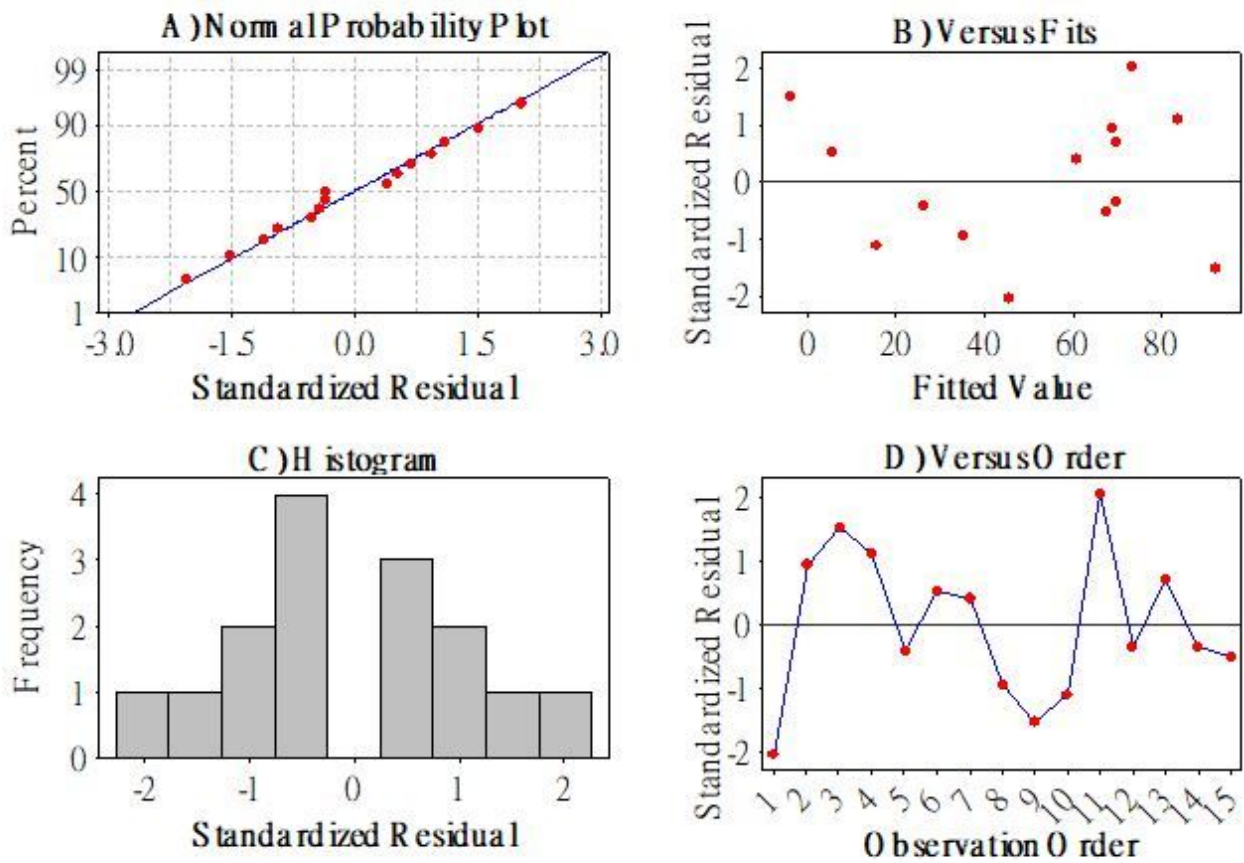


Figure 2

Standard error compared to A) standardized residual B) versus fits C) Histogram D) Versus Order. For DV30.

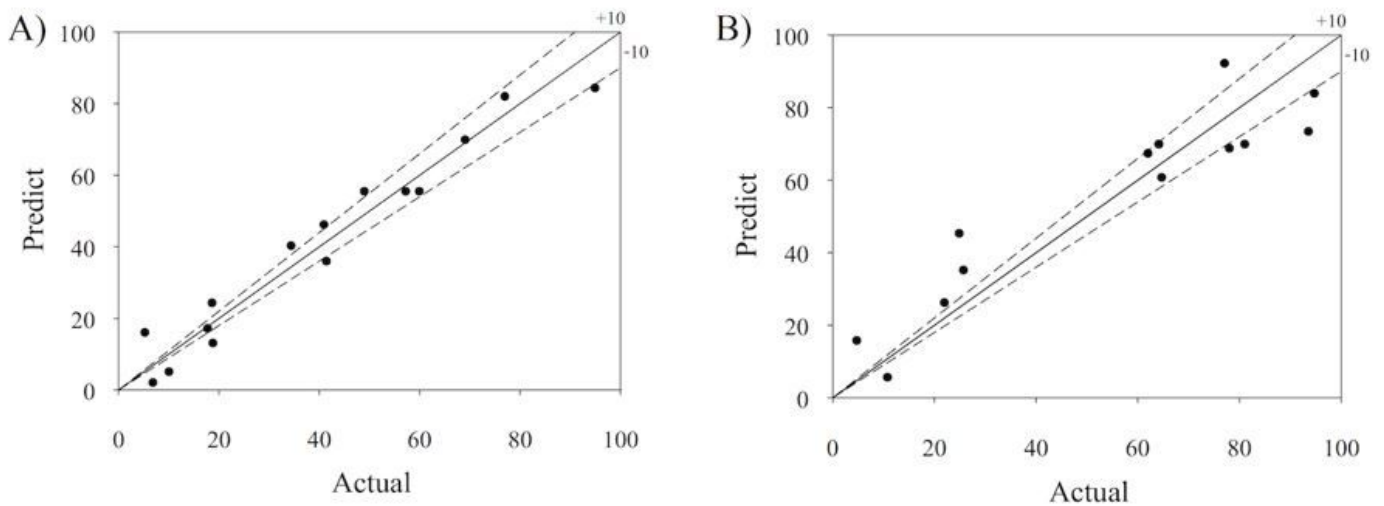


Figure 3

Experimental and predicted equation results for decolorization A) DR36 B) DV30

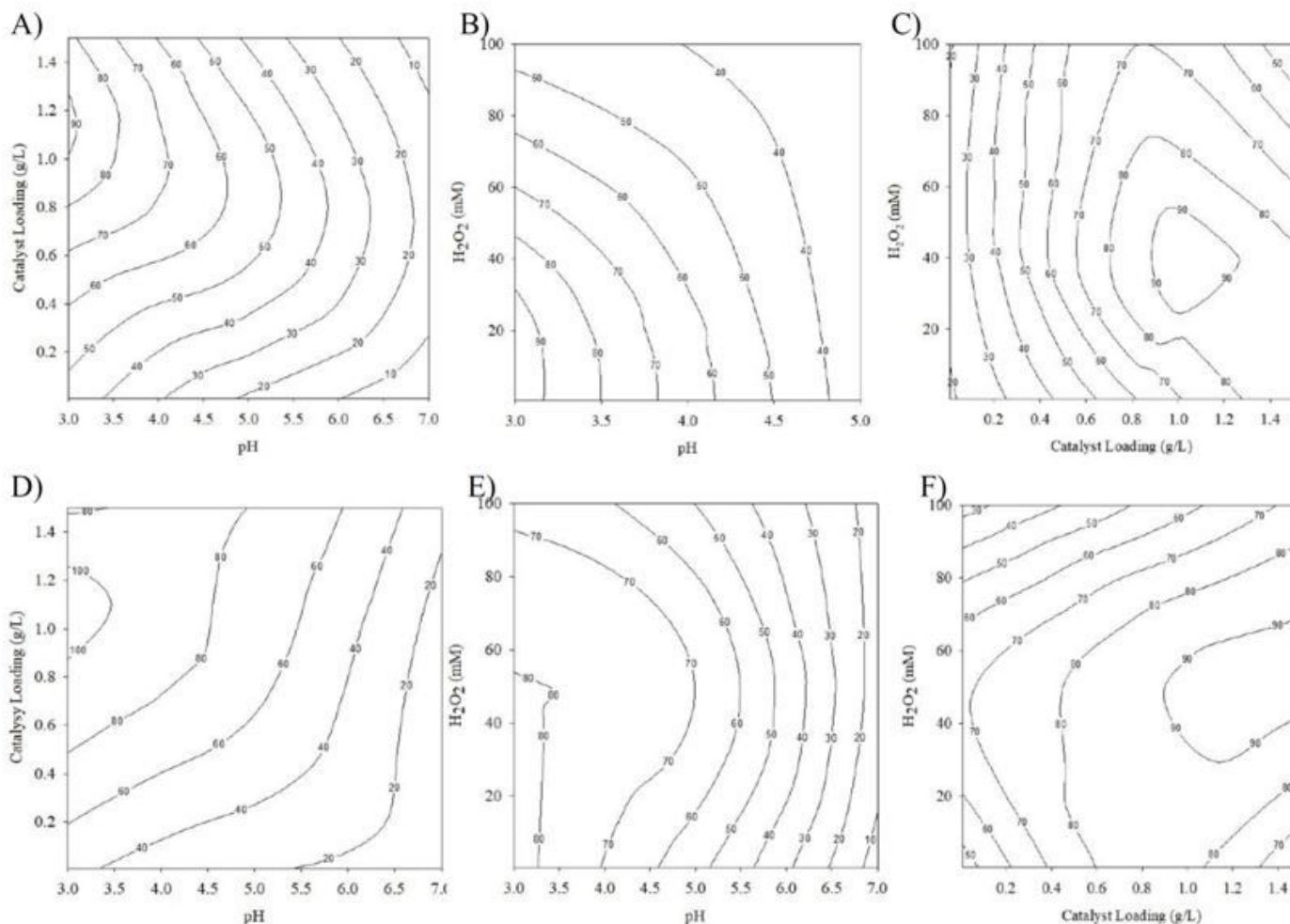


Figure 4

Contour plot illustrations, the interaction effect of variables on dye decolorization efficiency in the Fenton-like process in white (A-C) For DR36 and (D-F) for DV30.

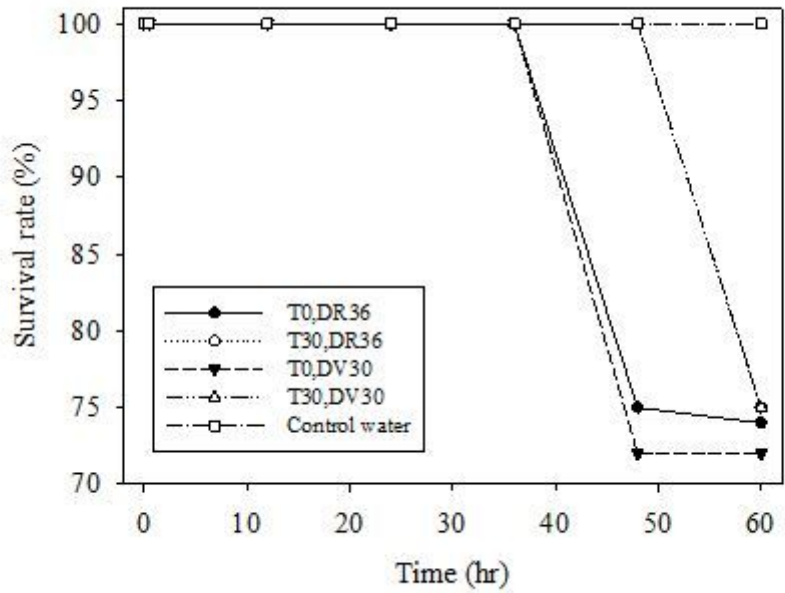


Figure 5

Effects of different treated water and untreated water with survival rate (%) of fairy shrimp (T0 is original dye at 300 ppm, T30 is treated water, and control water is water from a freshwater fairy shrimp)

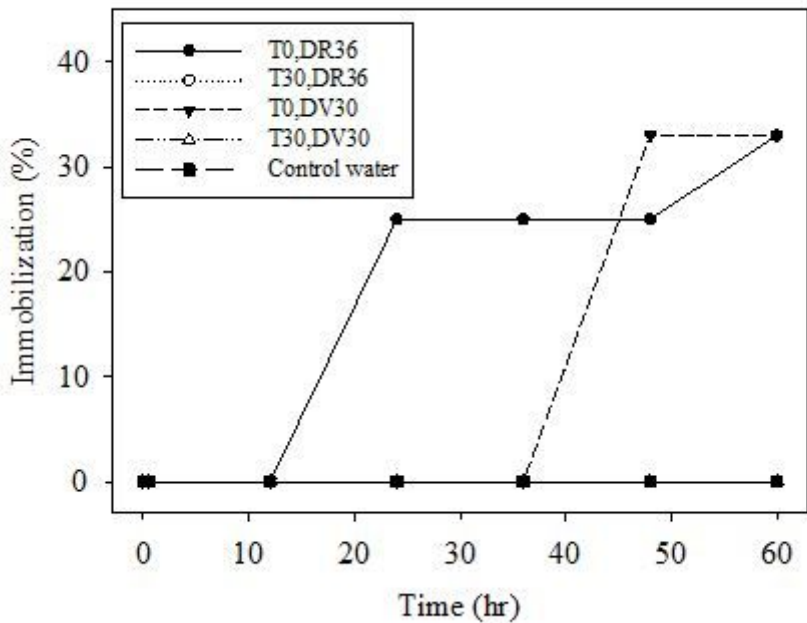


Figure 6

Effects of different treated water and untreated water with immobilization (%) of fairy shrimp, T0 is original dye at 300 ppm, T30 is treated water, and control water is water from a freshwater fairy shrimp culture